Biallelic *TRIP13* mutations predispose to Wilms tumor and chromosome missegregation

Shawn Yost[1*], Bas de Wolf[2*], Sandra Hanks[1*], Anna Zachariou[1], Chiara Marcozzi[3,4], Matthew Clarke[1], Richarda de Voer[2], Banafsheh Etemad[2], Esther Uijttewaal[2], Emma Ramsay[1], Harriet Wylie[1], Anna Elliott[1], Susan Picton[5], Audrey Smith[6], Sarah Smithson[7], Sheila Seal[1], Elise Ruark[1], Gunnar Houge[8], Jonathan Pines[3,4], Geert J.P.L. Kops[2,9,10+], Nazneen Rahman[1,11+]

[1] Division of Genetics and Epidemiology, Institute of Cancer Research, 15 Cotswold Road, London, SM2 5NG, UK

[2] Hubrecht Institute – KNAW (Royal Netherlands Academy of Arts and Sciences), Uppsalalaan 8, 3584 CT Utrecht, The Netherlands.

[3] The Gurdon Institute and Department of Zoology, University of Cambridge, Cambridge CB2 1QN, UK and [4] Division of Cancer Biology, The Institute of Cancer Research, 237 Fulham Road, London SW3 6JB, UK

[5] Children's and Adolescent Oncology and Haematology Unit, Leeds General Infirmary, Leeds, LS1 3EX, UK

[6] Yorkshire Regional Clinical Genetics Service, Chapel Allerton Hospital, Chapeltown Road, Leeds, LS7 4SA, UK

[7] Clinical Genetics Service, St Michael's Hospital, Southwell Street, Bristol, BS2 8EG, UK

[8] Center for Medical Genetics, Haukeland University Hospital, N-5021 Bergen, Norway

[9] Cancer Genomics Netherlands, and [10] Center for Molecular Medicine, University Medical Center Utrecht, 3584 CG, Utrecht, The Netherlands.

[11] Cancer Genetics Unit, Royal Marsden NHS Foundation Trust, London, UK SM2 5PT, UK

[*] These authors made equal contributions

[+] Joint senior authors

Correspondence should be addressed to
Nazneen Rahman email: rahmanlab@icr.ac.uk or Geert Kops email: g.kops@hubrecht.eu

Through exome sequencing we identified six individuals with biallelic loss-of-function mutations in *TRIP13*. All six developed Wilms tumor. Constitutional mosaic aneuploidies, microcephaly, developmental delay and seizures, which are features of mosaic variegated aneuploidy (MVA) syndrome[1,2], were more variably present. Through functional studies we show that *TRIP13*-mutant patient cells have no detectable TRIP13, and have substantial impairment of the spindle assembly checkpoint (SAC) leading to a high rate of chromosome missegregation. Accurate segregations as well as SAC proficiency are rescued by restoring TRIP13 function. Individuals with biallelic *TRIP13* or *BUB1B* mutations have a high risk of embryonal tumors[3], and here we show that their cells show severe SAC impairment. MVA due to biallelic *CEP57* mutations[4], or of unknown cause, is not associated with embryonal tumors and their cells show minimal SAC deficiency. These data suggest it may be the underlying mechanism leading to aneuploidy, rather than aneuploidy per se, that causes the high cancer risk associated with MVA syndrome, and provide insights into the complex relationships between aneuploidy and carcinogenesis.

Accurate chromosome segregation during cell division is required to maintain the correct number of chromosomes in cells. Errors of chromosome segregation can lead to aneuploidy, a term that describes cells with loss or gain of one or more chromosomes. Aneuploidy is an important cause of human disease, implicated in diverse pathologies, including recurrent miscarriage, infertility, developmental disorders and cancer[5-7]. Many biological processes, including spindle assembly, chromatid-spindle attachment, attachment error-correction, and the spindle assembly checkpoint (SAC) are involved in ensuring chromosome segregation proceeds flawlessly and that aneuploidy is prevented[6,8].

Rare individuals with constitutional mosaic aneuploidies involving varying chromosomes are well documented[1,2]. Affected individuals often have other clinical features such as microcephaly,

developmental delay and various congenital abnormalities, and the term 'mosaic variegated aneuploidy (MVA)' is used to describe this condition[1-3]. Cancer predisposition is one of the most important associations of MVA, with substantial increased risk of childhood malignancies, particularly Wilms tumor and rhabdomyosarcoma[3,9,10].

We have been studying this rare condition for over a decade. We previously reported biallelic mutations in the spindle assembly checkpoint gene *BUB1B* as a cause of MVA and childhood cancer[3]. To date we have identified 14 individuals with biallelic *BUB1B* mutations. More recently we identified biallelic mutations in *CEP57*, which encodes a centrosomal protein involved in kinetochore attachment, in four individuals with MVA, none of whom have developed cancer[4]. Together these two genes only account for a proportion of MVA cases.

To identify additional MVA genes we undertook exome sequencing in 43 individuals from 20 families, including 21 probands with MVA (Supplementary Table 1). We generated exome data using Illumina exome capture assays and called variants using the OpEx pipeline as previously described[11,12]. We performed two analyses to prioritize variants for further evaluation. We undertook an individual proband analysis to identify genes with two rare variants, as MVA is a recessively inherited condition. We also identified genes with protein truncating variants (PTVs) present in more than one proband, using the PTV prioritization method[4,12].

We identified the homozygous stop-gain mutation *TRIP13* c.1060C>T_p.Arg354X in three probands (ID_0319, ID_0644, ID_7054) (Table 1, Supplementary Fig. 1). The mutation leads to nonsense-mediated mRNA decay (Supplementary Fig. 2) and absence of detectable TRIP13 protein (Supplementary Fig. 3). Protein expressed from exogenous cDNA was degraded by the proteasome (Supplementary Fig. 4), suggesting that if any residual mRNA remains and is translated, mutant TRIP13 protein will not be expressed.

The three individuals had been independently recruited and there was no known relationship between them, but they were from families of Asian origin. Interestingly, all three had Wilms tumor. To further explore the association of *TRIP13* and Wilms tumor we performed exome sequencing in 11 UK individuals of reported Asian origin with Wilms tumor. Two, ID_0649 and ID_6112, were also homozygous for *TRIP13* c.1060C>T_p.Arg354X (Table 1 and Supplementary Fig. 1). ID_0649 had been noted to have premature chromatid separation, but no mosaic aneuploidies in lymphocytes. No constitutional karyotype in ID_6112 has been performed, but the tumor karyotype was reported to be normal. Of note, the sister of ID_6112 died at four years of age after developing a pelvic Sertoli-Leydig cell tumor and acute myeloid leukemia (AML). No sample is available for mutation testing, but this observation suggests biallelic *TRIP13* mutations may also predispose to cancers other than Wilms tumor.

The four available parental samples were all heterozygous for the mutation, consistent with recessive inheritance. The mutation is not present in the Exome Aggregation Consortium (ExAC) or ICR1000 series[13,14], nor is it present in 11,677 other exomes we have analyzed with the same pipeline. Multidimensional scaling analysis strongly suggests the families originate from Pakistan (Supplementary Fig. 5). Exploration of the available family history suggests the families come from the Azad Kashmir region of Pakistan. Many Azad Kashmir families were given work permits for the UK in the 1960s due to the construction of the Mangla Dam, which led to large-scale local displacement. The incidence of Wilms tumor in this region of Pakistan is very high (M Rashid, personal communication). This may be related to the *TRIP13* mutation we have identified. Evaluation of the contribution of the *TRIP13* mutation to Wilms tumor in this population would therefore be of interest.

We subsequently became aware of a Norwegian girl, ID_7679, who developed Wilms tumor at 15 months, who is homozygous for a different truncating *TRIP13* mutation. The mutation, c.697-

1G>C, is predicted to disrupt the canonical 3' splice-site in intron 7 of *TRIP13* and a new splice-site 2bp upstream is predicted to be used, resulting in a 2bp frameshift and premature protein truncation. No constitutional mosaic aneuploidies were observed in her lymphocytes.

These data provide compelling genetic evidence that *TRIP13* is a cancer predisposition gene. Biallelic loss-of-function *TRIP13* mutations confer a high risk of Wilms tumor and also predispose to chromosome segregation dysfunction which can manifest as mosaic aneuploidies and/or premature chromatid separation. There were no consistent phenotypic features amongst the six probands, though developmental delay, microcephaly, seizures, growth retardation and skin pigmentation were each noted in more than one individual (Table 1 and Supplementary Fig. 1).

TRIP13 encodes a highly conserved AAA+ATPase that contributes to homologue pairing, synapsis and recombination during meiosis[15]. In mitosis, TRIP13 promotes the conversion of the crucial SAC effector MAD2 to an inactive conformation via interaction with p31[comet 16,17]. This has dual impact on SAC function: in prometaphase, the generation of inactive MAD2 molecules enables continuous replenishment of MAD2 pools that can be activated by unattached kinetochores, thus ensuring long-term SAC signaling. In metaphase however, when no new active MAD2 is generated by kinetochores, MAD2 inactivation by TRIP13 causes SAC silencing and allows mitotic exit[18-20].

We sought to examine which defective molecular processes underlie aneuploidy and chromosome missegregation in *TRIP13*-mutant patients. We first infected immortalized *TRIP13*-mutant patient lymphoblasts with virus carrying H2B-mNeon to visualize chromatin. Live cell imaging showed that patient lymphoblasts displayed high levels of chromosome segregation errors such as lagging chromosomes and chromosome bridges (Fig. 1a,b). To understand how *TRIP13* mutations cause chromosomal instability (CIN) in patient cells, we examined the fidelity

of the SAC, the main chromosome segregation surveillance mechanism in which TRIP13 has been implicated. To this end, we analyzed cells for their ability to maintain mitotic arrest after exposure to the spindle poison nocodazole (Fig. 1c). Control cells maintained the arrest for >2 hours, whereas all cells from two different *TRIP13*-mutant patients escaped the arrest within one hour (Fig. 1c,d). Mitotic exit despite unattached chromosomes is indicative of a compromised SAC.

To gain insight into the molecular defect causing SAC impairment, we analyzed SAC protein expression and subcellular localization. Immunofluorescence imaging of the SAC effector MAD2 in nocodazole-treated cells showed that *TRIP13*-mutant patient cells recruited ~50% fewer molecules of MAD2 to their unattached kinetochores (Fig. 1e,f). Kinetochore levels of the MAD2 receptor MAD1 were unaffected (Fig. 1g). Absence of TRIP13 caused increased overall $p31^{comet}$ expression and reduced overall MAD2 expression (Supplementary Fig. 6), consistent with data reported in *TRIP13* knockout HeLa cells[20].

We next restored TRIP13 function by expressing GFP-TRIP13 in patient lymphoblasts using lentiviral delivery. Importantly, GFP-TRIP13 expression rescued the CIN as well as the SAC defect (Fig. 2a,b). Moreover, GFP-tagged TRIP13 p.Arg354X was unable to rescue an impaired SAC caused by CRISPR/Cas9-mediated knock out of the *TRIP13* gene in HCT116 cells (Fig. 2c and Supplementary Fig. 7,8). These observations provide an explanation for the chromosome segregation defects observed in individuals with biallelic *TRIP13* loss-of-function mutations. They also show that the SAC defects and resulting CIN are directly due to the loss of TRIP13 function caused by the homozygous *TRIP13* c.1060C>T_p.Arg354X mutation.

TRIP13 and BUBR1 (the protein encoded by *BUB1B*) are close functional partners in the spindle assembly checkpoint[15]. BUBR1 is part of the anaphase inhibitory complex MCC which also includes MAD2, the main target of TRIP13's remodeling activity in mitosis[21]. Notably,

severe SAC impairment was observed in *TRIP13*-mutant or *BUB1B*-mutant patient cells but not in cells from patients with *CEP57* mutations or in whom the cause of MVA remains unclear after exome sequencing (Fig. 3).

All six children with biallelic *TRIP13* mutations developed Wilms tumor in childhood, five of whom were successfully treated (Table 1). Limited information is available, but there were no obvious distinctive histopathological features in the tumors. Individuals with biallelic *BUB1B* mutations are also at high risk of childhood embryonal tumors. In fact, all MVA cases with childhood solid tumors in our series have either *BUB1B* or *TRIP13* mutations. By contrast, only one MVA individual in our series without mutations in *BUB1B* or *TRIP13* has developed cancer, an ALL at 3 years in a child in whom the cause of MVA remains unknown[10]. It is therefore tempting to speculate that the high cancer risk may be causally related to severe impairment of the SAC. Irrespective of the mechanism, our findings have clinical utility indicating that *BUB1B* and *TRIP13* mutation-positive individuals are at high risk of cancer and require close surveillance, whereas other individuals with MVA may be at lower cancer risk.

The data also suggest that the mechanism generating aneuploidy in affected individuals determines the cancer risk, not the aneuploidy per se. If confirmed, this is an important distinction as there has long been a debate regarding whether aneuploidy is a cause or consequence of cancer[5]. Further studies into the biological sequelae of these rare human mutations may therefore provide insights into the complex relationships between aneuploidy and carcinogenesis.

REFERENCES

1. Garcia-Castillo, H., Vasquez-Velasquez, A.I., Rivera, H. & Barros-Nunez, P. Clinical and genetic heterogeneity in patients with mosaic variegated aneuploidy: delineation of clinical subtypes. *Am J Med Genet A* **146a**, 1687-95 (2008).
2. Warburton, D., Anyane-Yeboa, K., Taterka, P., Yu, C.Y. & Olsen, D. Mosaic variegated aneuploidy with microcephaly: a new human mitotic mutant? *Ann Genet* **34**, 287-92 (1991).
3. Hanks, S. *et al.* Constitutional aneuploidy and cancer predisposition caused by biallelic mutations in BUB1B. *Nat Genet* **36**, 1159-61 (2004).
4. Snape, K. *et al.* Mutations in CEP57 cause mosaic variegated aneuploidy syndrome. *Nat Genet* **43**, 527-9 (2011).
5. Ricke, R.M. & van Deursen, J.M. Aneuploidy in health, disease, and aging. *J Cell Biol* **201**, 11-21 (2013).
6. Holland, A.J. & Cleveland, D.W. Boveri revisited: chromosomal instability, aneuploidy and tumorigenesis. *Nat Rev Mol Cell Biol* **10**, 478-87 (2009).
7. Torres, E.M., Williams, B.R. & Amon, A. Aneuploidy: cells losing their balance. *Genetics* **179**, 737-46 (2008).
8. Thompson, S.L., Bakhoum, S.F. & Compton, D.A. Mechanisms of chromosomal instability. *Curr Biol* **20**, R285-95 (2010).
9. Kajii, T. *et al.* Cancer-prone syndrome of mosaic variegated aneuploidy and total premature chromatid separation: report of five infants. *Am J Med Genet* **104**, 57-64 (2001).
10. Jacquemont, S., Boceno, M., Rival, J.M., Mechinaud, F. & David, A. High risk of malignancy in mosaic variegated aneuploidy syndrome. *Am J Med Genet* **109**, 17-21; discussion 16 (2002).
11. Ruark, E. *et al.* OpEx - a validated, automated pipeline optimised for clinical exome sequence analysis. *Sci Rep* **6**, 31029 (2016).
12. Mahamdallie, S.S. *et al.* Mutations in the transcriptional repressor REST predispose to Wilms tumor. *Nat Genet*, 1471-1474 (2015).
13. Lek, M. *et al.* Analysis of protein-coding genetic variation in 60,706 humans. *Nature* **536**, 285-91 (2016).
14. Ruark, E. *et al.* The ICR1000 UK exome series: a resource of gene variation in an outbred population. *F1000Res* **4**, 883 (2015).
15. Vader, G. Pch2(TRIP13): controlling cell division through regulation of HORMA domains. *Chromosoma* **124**, 333-9 (2015).
16. Eytan, E. *et al.* Disassembly of mitotic checkpoint complexes by the joint action of the AAA-ATPase TRIP13 and p31(comet). *Proc Natl Acad Sci U S A* **111**, 12019-24 (2014).
17. Ye, Q. *et al.* TRIP13 is a protein-remodeling AAA+ ATPase that catalyzes MAD2 conformation switching. *Elife* **4**(2015).
18. Wang, K. *et al.* Thyroid hormone receptor interacting protein 13 (TRIP13) AAA-ATPase is a novel mitotic checkpoint-silencing protein. *J Biol Chem* **289**, 23928-37 (2014).

19. Nelson, C.R., Hwang, T., Chen, P.H. & Bhalla, N. TRIP13PCH-2 promotes Mad2 localization to unattached kinetochores in the spindle checkpoint response. *J Cell Biol* **211**, 503-16 (2015).

20. Ma, H.T. & Poon, R.Y. TRIP13 Regulates Both the Activation and Inactivation of the Spindle-Assembly Checkpoint. *Cell Rep* **14**, 1086-99 (2016).

21. Vleugel M, Hoogendoorn E, Snel B, Kops GJ. Evolution and function of the mitotic checkpoint. *Dev Cell* **23**, 239-50 (2012).

URLs

OpEx variant calling pipeline: www.icr.ac.uk/opex

ICR1000 UK exome series: www.icr.ac.uk/icr1000exomes

Exome Aggregation Consortium (ExAC): http://exac.broadinstitute.org.

1000 Genomes Project: ftp://ftp.1000genomes.ebi.ac.uk/vol1/ftp/release/20110521/

Acknowledgements

We thank the families for their participation and the researchers that recruited them including K. Asakura-Hay, S. Bernardo de Sousa, P. Callier, D. Chitayat, J. Clayton-Smith, S. Fernandes. D. FitzPatrick, L. Florentin, J. Hurst, B. Isidor, S. Jacquemont, R. Marin Iglesias, M. Micale, J. Tolmie. We thank H.J. Snippert for providing the Lentiviral H2B plasmid. We thank Anthony Renwick, Shazia Mahamdallie, Chey Loveday and members of the Kops lab for helpful discussions and Ann Strydom and Brittany Rex for assistance in preparing the manuscript. We acknowledge NHS funding to the Royal Marsden/ICR NIHR Biomedical Research Centre. This research was supported by the Wellcome Trust (100210/Z/12/Z), by the Netherlands Organisation for Scientific Research (NWO-ALW 823.02.004 to GJPLK) and by the Dutch Cancer Society (KWF Kankerbestrijding to RdV).

Author contributions

N.R. designed and oversaw the study. G.K designed and oversaw the functional experiments. E. Ra. undertook the exome sequencing. S.H., H.W. and S.Se. performed the molecular analyses. S.Y., M.C., and E.Ru. performed bioinformatic analyses. B.dW., E.U., R.dV., B.E. and C.M. undertook functional analyses under the supervision of G.K., and J.P. S.P., A.S., S.Sm. provided samples and data, coordinated by A.Z. and A.E. S.Y., S.H., B.dW., A.Z., G.K. and N.R. wrote the paper with input from the other authors.

Competing financial interests

The authors declare that they have no competing financial interests.

Figure Legends

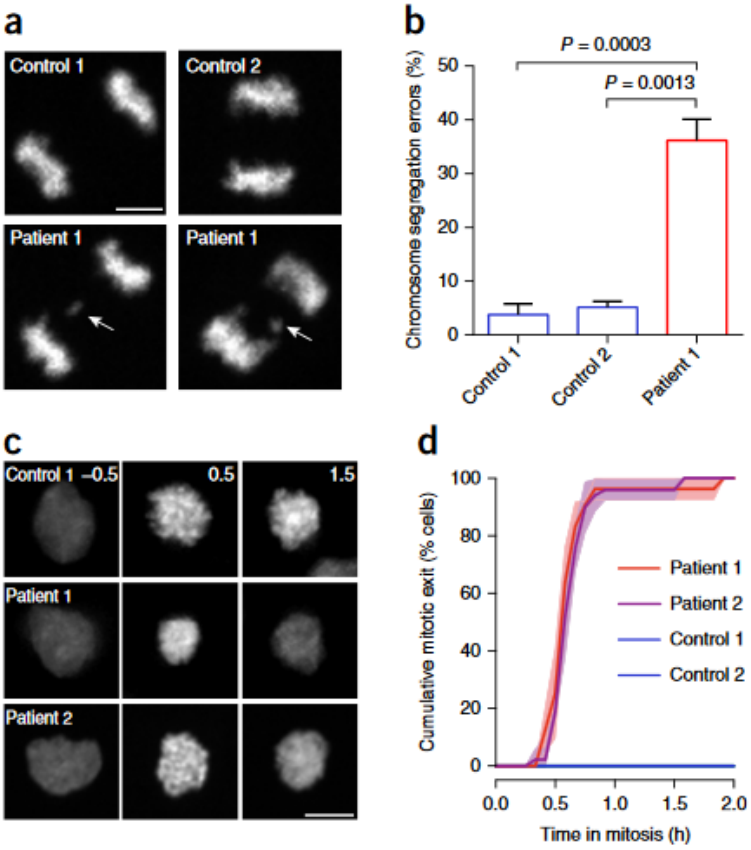

Figure 1: *TRIP13* loss-of-function mutations cause chromosome segregation errors and SAC deficiency

(a) Representative anaphases of immortalized control (upper) and *TRIP13*-mutant patient (lower) lymphoblasts expressing H2B-mNeon, showing a lagging chromosome in the lower panel.

(b) Quantification of chromosome segregation errors of lymphoblasts as visualized in (a). Each bar depicts the mean of 3-4 experiments ±SEM, >60 cells in total. P-values ≤ 0.05, from unpaired Student's t-tests, are shown. Patient 1 cells show increased levels of chromosome segregation errors.

(c) Representative images of H2B-mNeon expressing control (upper) and patient (lower) lymphoblasts going through mitosis (time in hours with mitotic entry at t=0.0) in the presence of nocodazole. Only the patient 1 cell has exited from mitosis after 1.5 hours (lower right panel).

(d) Analysis of mitotic delay of cells as visualized in (c), indicating the cumulative percentage of cells that exited from mitosis as a function of time (mean of three experiments ±SEM, 10-30 cells per experiment). Both patient cell lines escaped mitotic arrest within one hour.

(e-g) Immunofluorescence labelling (e) and quantification (f-g) of indicated proteins in nocodazole-arrested control or patient lymphoblasts. Each dot represents one cell, with dots from separate experiments in different shades of grey. The red bar depicts the mean of four experiments ±SEM, >70 cells in total. P-values ≤ 0.05, from unpaired Student's t-tests, are shown. Patient 1 cells have reduced kinetochore levels of MAD2, but not MAD1, compared to the controls.

Key: patient 1, ID_0644; patient 2, ID_7054; SEM, standard error of the mean

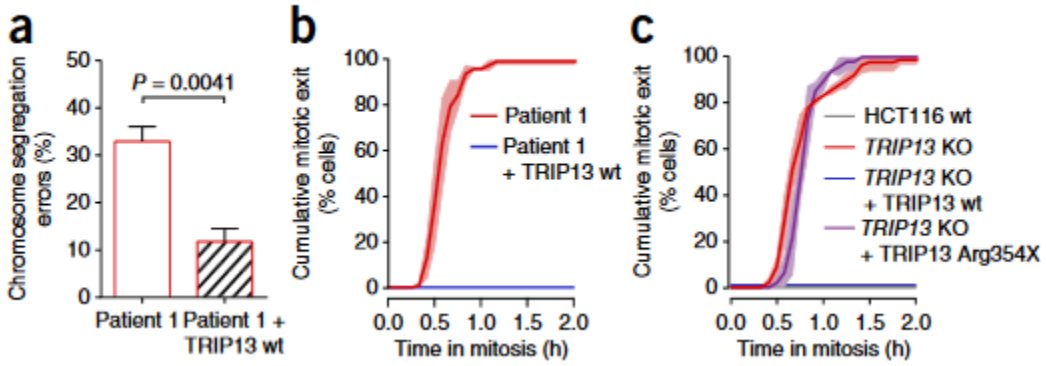

Figure 2: SAC deficiency and CIN caused by *TRIP13* loss-of-function is rescued with wild type TRIP13

(a) Quantification of chromosome segregation errors of TRIP13-mutated patient lymphoblasts expressing H2B-mNeon or co-expressing LAP-TRIP13 wt. Each bar depicts the mean of 3-4 experiments ±SEM, >85 cells in total. P-values ≤ 0.05 from an unpaired Student's t-test are shown. Addition of LAP-TRIP13 wt to patient 1 cells reduced the rate of chromosome missegregation.

(b) Analysis of mitotic delay as in (Fig 1d) of nocodazole-treated patient lymphoblasts expressing H2B-mNeon or co-expressing GFP-TRIP13 wt. Mean of three experiments ±SEM, >35 cells in total. Patient 1 cells expressing GFP-TRIP13 now maintain mitotic arrest.

(c) Analysis of mitotic delay as in (Fig 1d) and (b) of nocodazole-treated HCT116 wt or HCT116 TRIP13 KO cells expressing H2B-mNeon, co-expressing GFP-TRIP13 wt, or co-expressing TRIP13 p.Arg354X. Mean of three experiments ± SEM, >45 cells in total. HCT116 wt and TRIP13 KO + TRIP13 wt cells both maintain mitotic arrest unlike TRIP13 KO and TRIP13 KO + TRIP13 p.Arg354X cells.

Key: patient 1, ID_0644; wt, wild-type; KO, knockout; CIN, chromosomal instability; SAC, spindle assembly checkpoint; SEM, standard error of the mean

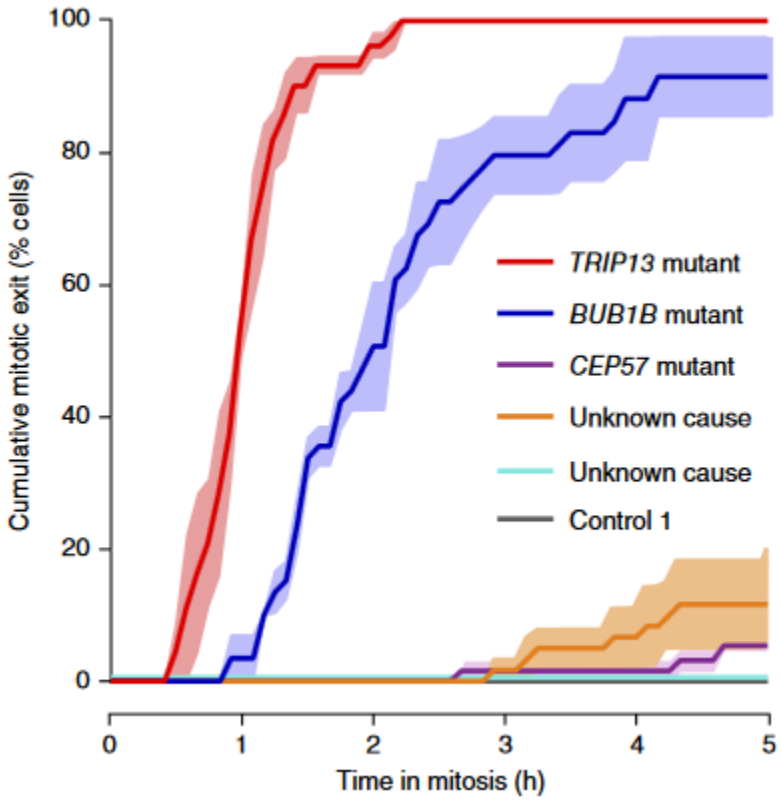

Figure 3: Patient cells with TRIP13 or BUB1B mutations have severely compromised SAC
Analysis of mitotic delay as in Fig 1d and Fig 2b of nocodazole-treated MVA patient lymphoblasts treated with far-red DNA dye to visualize the DNA, showing the cumulative percentage of cells that exited from mitosis as a function of time (mean of three experiments ±SEM, 20 cells per experiment). Only TRIP13-mutant or BUB1B-mutant patient cells rapidly escape from mitotic arrest.
Key: SAC, spindle assembly checkpoint; SEM, standard error of the mean

Table 1 Summary of molecular and clinical findings in individuals with biallelic *TRIP13* mutations

ID	TRIP13 mutations	Aneuploidy	Premature chromatid separation	Wilms tumor age at diagnosis	Current status	Other clinical features
ID_0319	c.1060C>T_p.Arg354X c.1060C>T_p.Arg354X	yes	uk	2 yrs	alive, 6 yrs	microcephaly, developmental delay, growth retardation arthrogryposis,
ID_0644	c.1060C>T_p.Arg354X c.1060C>T_p.Arg354X	yes	yes	4 yrs, relapse 5 yrs	alive, 43 yrs	growth retardation
ID_7054	c.1060C>T_p.Arg354X c.1060C>T_p.Arg354X	yes	yes	2 yrs	alive, 5 yrs	*café au lait* patches
ID_0649	c.1060C>T_p.Arg354X c.1060C>T_p.Arg354X	no	yes	2 yrs relapse 10 yrs	died, 10 yrs	microcephaly, growth retardation, seizures, skin pigmentation
ID_6112	c.1060C>T_p.Arg354X c.1060C>T_p.Arg354X	uk	uk	5 yrs	alive, 6 yrs	
ID_7679	c.673-1G>C c.693-1G>C	no	uk	1.3 yrs	alive, 1.5 yrs	seizures, developmental delay

Fuller details are provided in Supplementary Fig 1.